TURBULENT FLOW IN THE NEAR-WALL REGION AS ANISOTROPIC-FLUID FLOW

V. A. Babkin   UDC 532.517.4

A model of near-wall turbulent flow of an incompressible Newtonian fluid has been constructed. The model is based on the anisotropy of the turbulent flow. Theoretical and experimental results have been compared.

It is well known [1–8] that the character of turbulent flow near a solid wall is determined by the vortical structure inherent in it. As for the latter, according to [4–8], it consists of so-called Λ-vortices which fill the near-wall region densely. A Λ-vortex has a crest — a point of the vortex most distant from the wall — and two branches going toward the side opposite to the direction of flow. With distance from the crest the branches approach the wall, aligning with the flow. Although the crests of isolated Λ-vortices can considerably deviate from the wall, the overwhelming part of them lies in the region which is generally termed near-wall. Due to the structuring by the vortices, the turbulent flow becomes anisotropic [1–9].

A number of models of turbulent flow which are based on its structural properties were developed [3, 6–8, 10–13] for adequate description of the experimentally observed properties of flow anisotropy. However, experimental verification and practical use of general models are difficult due to both the complexity of the governing equations and the large number of unknown characteristic constants. To get around these difficulties, below we suggest a model for description of a narrower class of turbulent flows, i.e., near-wall ones. A specific feature of the model is that it involves, as the characteristic parameter, the so-called landmark vector which determines the physical properties of a moving medium at each point [14–17].

The landmark vector was first used in [10] to characterize eddy viscosity. Then, in [11], it was shown that based on the oriented-fluid model [14–16] one can obtain a logarithmic velocity profile for incompressible-fluid flow between parallel plane walls. Somewhat later, in [12, 13], a rather general theory of turbulence, with the landmark vector being one of its main kinematic parameters, was developed.

Although the theoretical conclusions of the above studies are confirmed by experimental results, use of the landmark vector in them is hypothetical in character, since the same experimental results can be explained within the framework of different theories. However, it has been shown recently in [9] that at each point of near-wall turbulent flow there exists a direction which affects turbulent stresses and links between them. Owing to the relations between turbulent stresses found in [9], the equations of state of the model can be verified already at the stage of formulation. In light of the facts revealed in [9], the study of near-wall turbulence with account for flow anisotropy seems rather promising.

1. Equations of Motion and State. In view of the wave structure in the near-wall region of the turbulent flow, the moving fluid at each point of this region will be considered as a transversely isotropic medium whose determining parameters include the landmark vector. The equations of state and motion of these fluids were first obtained in [14, 15] (Ericksen–Leslie model). Although this model was constructed for the description of liquid crystals, it has no elements typical of solely liquid crystals; therefore, it will be used in this case also.

Assuming that the fluid is incompressible and flow is isothermal, in the Cartesian coordinate system x_1, x_2, x_3 the equations of continuity and motion of the oriented fluid have the form [14, 17]

$$u_{\alpha,\alpha} = 0 \, , \tag{1}$$

$$\rho \dot{u}_i = p_{i\alpha,\alpha} + f_i \, , \tag{2}$$

$$I\ddot{n}_i = \beta_{i\alpha,\alpha} + g_i + G_i , \qquad (3)$$

The quantities β_{ij}, g_i, and G_i related to the change in the landmark vector are termed generalized. Hereinafter summation from 1 to 3 is assumed to be done over the double subscripts.

The stresses p_{ij} are considered as sums of the form

$$\dot{v} = \frac{dv}{dt}, \quad v_{,i} = \frac{\partial v}{\partial x_i}, \quad v = u_i, n_i, p_{ij}, \beta_{ij} .$$

$$p_{ij} = -\rho\delta_{ij} + \sigma_{ij} + \tau_{ij} . \qquad (4)$$

With closest applications of the model in mind, we restrict ourselves to an important particular case where the landmark vector n_i has a unit length. Then the equations of state can be represented in the form [14–17]

$$\sigma_{ij} = -\rho \frac{\partial F}{\partial n_{\alpha,j}} n_{\alpha,j} , \qquad (5)$$

$$\beta_{ij} = \alpha_j n_i + \rho \frac{\partial F}{\partial n_{i,j}} , \qquad (6)$$

$$\tau_{ij} = \mu_1 n_\alpha n_\beta e_{\alpha\beta} n_i n_j + \mu_2 N_i n_j + \mu_3 N_j n_i + \mu_4 e_{ij} + \mu_5 n_i n_\alpha e_{\alpha j} + \mu_6 n_j n_\alpha e_{\alpha i} , \qquad (7)$$

$$g_i = \gamma n_i - (\alpha_\beta n_i)_{,\beta} + \lambda_1 N_i + \lambda_2 n_\alpha e_{i\alpha} - \rho \frac{\partial F}{\partial n_i} , \qquad (8)$$

$$e_{ij} = \frac{1}{2}(u_{i,j} + u_{j,i}), \quad \omega_{ij} = \frac{1}{2}(u_{i,j} - u_{j,i}), \quad N_i = \dot{n}_i - \omega_{i\alpha} n_\alpha . \qquad (9)$$

Here F for liquid nematic crystals is assigned in the simplest form by the formula [14–17]

$$2\rho F = 2\rho F_0 + k_{22} n_{\alpha,\beta} n_{\alpha,\beta} + k_{24} n_{\alpha,\beta} n_{\beta,\alpha} + (k_{11} - k_{22} - k_{24}) n_{\alpha,\alpha}^2 + (k_{33} - k_{22}) n_\alpha n_\beta n_{\gamma,\alpha} n_{\gamma,\beta} . \qquad (10)$$

The scalar function γ and the vector function α_i are introduced into the equations of state to provide the consistency of the model in the case of an incompressible fluid and a constant landmark vector. If the fluid is compressible and the landmark vector can have an arbitrary length, one should set $\gamma = \alpha_i = 0$, $i = 1, 2, 3$. A thermodynamic analysis [16, 17] leads to the following relations between the determining constants of the model:

$$k_{11} \geq |k_{11} - k_{22} - k_{24}| , \quad k_{22} \geq |k_{24}| , \quad k_{33} \geq 0 , \qquad (11)$$

$$\lambda_1 = \mu_2 - \mu_3 , \quad \lambda_2 = \mu_5 - \mu_6 = -(\mu_2 + \mu_3) , \quad -4\lambda_1(2\mu_4 + \mu_5 + \mu_6) \geq (\mu_2 + \mu_3 - \lambda_2)^2 , \quad \mu_4 \geq 0 ,$$

$$ \qquad (12)$$

$$2\mu_1 + 3\mu_4 + 2\mu_5 + 2\mu_6 \geq 0 , \quad 2\mu_4 + \mu_5 + \mu_6 \geq 0 .$$

Expecting to use the Ericksen–Leslie model for description of near-wall turbulent flows, let us assume that it, first of all, is in agreement with the well-substantiated experimental facts. It was found by numerous experiments that in turbulent fluid flow between parallel plane walls whose equations are $x_2 = \pm h$ (the x_1 axis is directed along the flow and the x_2 axis is perpendicular to the walls), the longitudinal averaged velocity u in the near-wall region has a logarithmic profile:

1093

$$\frac{u}{w_*} = \frac{1}{\kappa} \ln\left(1 - \frac{|x_2|}{h}\right) + C. \tag{13}$$

As is shown in [11], in order that in this flow the Ericksen–Leslie model lead to profile (13), it is necessary that, along with conditions (11) and (12), the constants of the model satisfy the equalities

$$k_{11} = k_{33} = 0, \quad k_{24} = -k_{22}, \quad \mu_2 = \mu_3 = 0. \tag{14}$$

Under these conditions, Eqs. (5)–(8) take the form

$$\sigma_{ij} = k_{22} n_{\alpha,i} (n_{j,\alpha} - n_{\alpha,j} + n_j n_\beta n_{\alpha,\beta}), \tag{15}$$

$$\beta_{ij} = \alpha_j n_i + k_{22} (n_{i,j} - n_{j,i} - n_j n_\alpha n_{i,\alpha}), \tag{16}$$

$$g_i = \gamma n_i - (\alpha_\beta n_i)_{,\beta} + k_{22} n_\alpha n_{\beta,\alpha} n_{\beta,i}, \tag{17}$$

$$\tau_{ij} = \mu_1 n_\alpha n_\beta e_{\alpha\beta} n_i n_j + \mu_4 e_{ij} + \mu_5 n_\alpha (n_i e_{\alpha j} + n_j e_{\alpha i}). \tag{18}$$

We will consider them to be the governing equations of the viscous fluid in turbulent flow in the near-wall region.

The attempts made by us to obtain similar conditions of the logarithmic velocity profile on the basis of the model of [12, 13] have not met with success; therefore, we took the considered Ericksen–Leslie model as the basis.

The problem of physical interpretation of the landmark vector n_i in the case of anisotropic turbulence has not been unambiguously solved as yet. In [3], it was assumed that "viscous anisotropy is related to the orientation of the axes of turbulent formations," while in [12, 13], it is stated that the landmark vector is directed along the principal axis of the deformation-rate tensor determined by the field of averaged velocities, to which there corresponds the highest eigenvalue. By analogy with the theory of oriented fluids [14–17], it seems more natural to us to assume that the landmark vector characterizes the central direction of vortex lines at a point of the flow. In this case, the velocity of flow u_i and the landmark vector n_i, being related in terms of the equations of motion and state, are independent determining parameters of the model.

2. Analysis of the Model. Comparison with Experimental Results. Investigating plane turbulent flow of an incompressible fluid in the near-wall region, Zhang and Eisele [9] found and experimentally confirmed the following facts:

I. The direction of the velocity at a flow point is a random quantity and is characterized by the angle of slope of the random velocity to the fixed axis, e.g., the x_1 axis. The averaged value of this angle ψ is a function of the coordinates of the flow point.

II. The turbulent (Reynolds) stresses at the point of the steady-state flow t_{11}, t_{22}, and t_{12} (Cartesian coordinates x_1, x_2) are interrelated by the equality

$$t_{12} = \frac{1}{2}(t_{11} - t_{22})\tan 2\psi. \tag{19}$$

One principal axis of the stress tensor t_{ij} is tilted at an angle ψ to the x_1 axis.

III. If $(x_{1'}, x_{2'})$ is a system of Cartesian coordinates turned by the angle φ relative to the system (x_1, x_2), then the turbulent stresses $t_{1'1'}$ and $t_{1'2'}$ in the new axes are related to the stresses in the previous axes by the equalities

$$t_{1'1'} = \frac{1}{2}(t_{11} + t_{22}) + \frac{\cos 2(\varphi - \psi)}{2\cos 2\psi}(t_{11} - t_{22}), \quad t_{1'2'} = -\frac{\sin 2(\varphi - \psi)}{2\cos 2\psi}(t_{11} - t_{22}). \tag{20}$$

Let us find out to what measure the turbulent stresses of the model considered are in agreement with these facts. For the plane flow of the oriented fluid with a unit landmark vector n_i we have

1094

$$u_1 = u_1(x_1, x_2), \quad u_2 = u_2(x_1, x_2), \quad n_1 = \cos\theta, \quad n_2 = \sin\theta. \tag{21}$$

Since equalities (19) and (20) relate the stresses t_{ij} caused by turbulence, in the case of flow of the oriented fluid in formulas for stresses which we also denote as t_{ij}, we allow only for those terms which explicitly involve the landmark vector. Then it follows from formulas (15) and (18) that

$$t_{ij} = \sigma_{ij} + \tau_{ij} - \mu_4 e_{ij} = k_{22}n_{\alpha,i}(n_{j,\alpha} - n_{\alpha,j} + n_j n_\beta n_{\alpha,\beta}) + \mu_1(n_\alpha n_\beta e_{\alpha\beta} n_i n_j + \mu_5 n_\alpha(n_i e_{\alpha j} + n_j e_{\alpha i}). \tag{22}$$

Substitution of functions (21) into formula (22) yields explicit expressions for t_{ij}:

$$t_{11} = \mu_1 R(\theta)\cos^2\theta + \mu_5 \cos\theta\,[2u_{1,1}\cos\theta + (u_{1,2} + u_{2,1})\sin\theta],$$

$$t_{22} = \mu_1 R(\theta)\sin^2\theta + \mu_5 \sin\theta\,[2u_{2,2}\sin\theta + (u_{1,2} + u_{2,1})\cos\theta],$$

$$2t_{12} = 2t_{21} = \mu_1 R(\theta)\sin 2\theta + \mu_5\,[u_{1,2} + u_{2,1} + (u_{1,1} + u_{2,2})\sin 2\theta], \tag{23}$$

$$R(\theta) = u_{1,1}\cos^2\theta + (u_{1,2} + u_{2,1})\sin\theta\cos\theta + u_{2,2}\sin^2\theta.$$

Simple transformations of formulas (23) give the equality

$$2t_{12} = (t_{11} - t_{22})\tan 2\theta + \mu_5\,[u_{1,2} + u_{2,1} + (u_{2,2} - u_{1,1})\tan 2\theta], \tag{24}$$

which coincides with (19) if the angles ψ and θ are identified and it is assumed that $\mu_5 = 0$. Under the same conditions, the stresses t_{11}, t_{22}, and t_{12} determined by formulas (23) also satisfy equalities (20), which can easily be found by direct verification.

Since relations (19) and (20) are confirmed experimentally [9], we can consider that at this stage the model with equations of state (15)–(18), where (18) has the form

$$\tau_{ij} = \mu_1 n_\alpha n_\beta e_{\alpha\beta} n_i n_j + \mu_4 e_{ij} \tag{25}$$

is confirmed as well.

Next we find out how this model agrees with the known experiments [1]. For this purpose, we consider confined turbulent flow of an incompressible fluid between parallel plane walls. For the sake of convenience we take the conventional notation of the coordinates x, y: the x axis is along the flow and the y axis is perpendicular to the walls. The equations of the planes are $y = \pm h$.

Let the external mass forces f_i and G_i be absent in the equations of motion (2) and (3). Due to the flow symmetry we can seek the solution in the form

$$u_x = u(y), \quad u_y = u_z = 0, \quad n_x = \cos\theta(y), \quad n_y = \sin\theta(y), \quad n_z = 0. \tag{26}$$

Then (2) and (3) simultaneously with the equations of state (15)–(17) and (25) are reduced to

$$\left(\mu_1\sin^2\theta\cos^2\theta + \frac{\mu_4}{2}\right)u' = -\tau_w\frac{y}{h}, \quad \tau_w = -\frac{\partial p}{\partial x}h, \tag{27}$$

$$\sin\theta\cos\theta\,\theta'' + (1 - 3\sin^2\theta)\,\theta'^2 - \frac{\gamma}{k_{22}} = 0, \tag{28}$$

where the derivatives with respect to y are primed. Equation (28) is one of the two coincident equations which follow from (3) at an arbitrary γ, and hence γ does not affect the simultaneousness of these equations. Therefore, we set $\gamma = 0$. In this case, the boundary conditions are
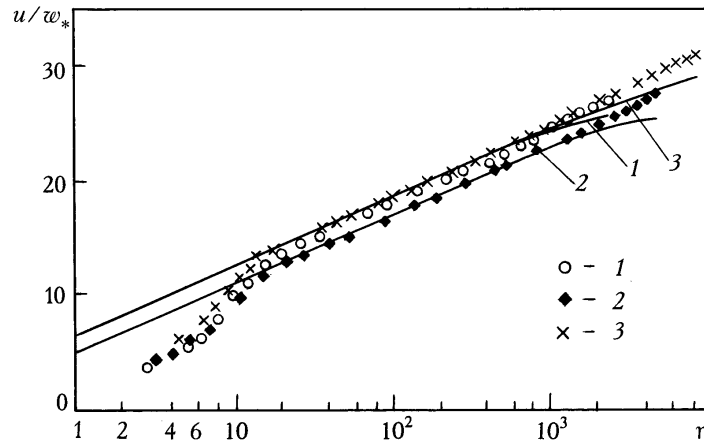
Fig. 1. Dimensionless velocity u/w_* as a function of dimensionless distance to the wall $\eta = (h - |y|)w_*/\nu$ in flow between parallel plane walls: curves, calculation from formula (31) [1) Re = 57,000; 2) 120,000; 3) 230,000]; dots, experiment [1].

$$\sin \theta \,(\pm h) = 0 \,, \quad u \,(\pm h) = 0 \,. \tag{29}$$

On the assumption that the landmark vector characterizes the direction of vortices locally, the first boundary conditions of (29) reflect the fact that near the wall Λ-vortices are extended along the flow [7].

The solution of the system of equations (27), (28) with (29) has the form [11]

$$\cos \theta = t \,, \quad t = [1 - 3 \sqrt{B} \,(h - |y|)]^{1/3} \,, \tag{30}$$

$$\frac{3\mu_1 hB}{\sqrt{\rho \tau_w}} \frac{u}{w_*} = \frac{3h \sqrt{B} - 1}{2q^2 - 1} \left[\sqrt{q^2 - 1} \, \arctan \frac{1}{\sqrt{q^2 - 1}} + \frac{q}{2} \ln \frac{q - t}{q + t} \right] +$$

$$+ \frac{1 + 2\alpha}{4\,(2q^2 - 1)} \ln \frac{q^2 - t^2}{t^2 + q^2 - 1} + \frac{1}{4} \ln \left| t^4 - t^2 - \alpha \right| + \frac{t^2}{2} + C \,, \tag{31}$$

$$C = \frac{1 - 3h \sqrt{B}}{2q^2 - 1} \left[\sqrt{q^2 - 1} \, \arctan \frac{1}{\sqrt{q^2 - 1}} + \frac{q}{2} \ln \frac{q - 1}{q + 1} \right] - \frac{1 + 2\alpha}{4\,(2q^2 - 1)} \ln \left(1 - \frac{1}{q^2} \right) - \frac{\ln \alpha}{4} - \frac{1}{2} \,, \tag{32}$$

$$2\alpha = \mu_4/\mu_1 \,, \quad 2q^2 = 1 + \sqrt{1 + 4\alpha} \,, \quad q > 0 \,.$$

The constant B is determined by the formula

$$B = \theta_0'^2 \sin^2 \theta_0 \cos^4 \theta_0 \,, \tag{33}$$

where θ_0 and θ_0' are the values of the angle of slope of the landmark vector and its derivative on the upper boundary of the vortical layer $y = \pm(h - \delta)$. On the basis of equality (33), the near-wall layer is determined as the layer structurized by vortices.

In addition to the solution (30)–(33), Eq. (28) at $\gamma = 0$ and with the first boundary condition of (29) also has the solution $\theta(y) = 0$. Substitution of it into (27) converts the latter to the equation of laminar flow; therefore, we restrict ourselves to consideration of the solution (30)–(33).

TABLE 1. Experimental Data [1] and the Values of the Parameters Used for Obtaining Curves in Fig. 1

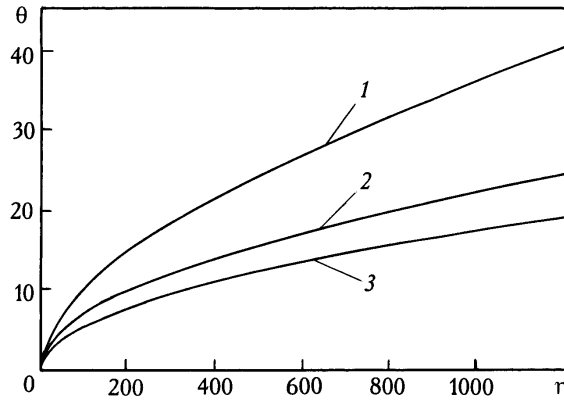| Re	w_*, m/sec	μ_1, kg/(m·sec)	μ_4, kg/(m·sec)	B, m^2	δ/h
57,000	0.39	0.021	$1.43 \cdot 10^{-6}$	16.8	0.51
120,000	0.80	0.047	$2.44 \cdot 10^{-6}$	14.5	0.25
230,000	1.36	0.073	$1.49 \cdot 10^{-6}$	17.0	0.15

Fig. 2. Angle of slope of the landmark vector θ to the x axis as a function of dimensionless distance to the wall η in flow between parallel plane walls: 1–3, the same as in Fig. 1.

Figure 1 shows experimental points [1] and calculated curves of the solution (30)–(33) under experimental conditions [1]. The test fluid is air at $\rho = 1.205$ kg/m^3 and $\nu = 1.500 \cdot 10^{-5}$ m^2/sec. The distance between the planes is $2h = 0.18$ m. The values of the calculated parameters are given in Table 1. It follows from the graphs that in the region $\eta \geq 20$, where $\eta = (h - |y|)w_*/\nu$, the solution (30)–(33) agrees with the experimental data no worse than the universal logarithmic law [1, 18], whereas directly near the wall, the calculated and experimental results differ greatly. When $\eta < 20$, flow turbulization of the flow is weakened considerably, the flow becomes less anisotropic and other models are needed for adequate description of it (e.g., models of viscous laminar and transition sublayers [18]).

The extreme right points of curves 1–3 correspond to $t = 0$. Formally they determine the upper limit of near-wall turbulent flow. However, the experimental points begin to deviate from the calculated curves somewhat earlier, at about $\eta = 1200$. It would appear natural to take the distance from the wall $(h - y)$ which corresponds to this value of η as the thickness of the near-wall turbulent region δ. The ratios δ/h at different Reynolds numbers are given in Table 1. The thickness of the region decreases as the flow velocity increases.

Figure 2 shows the plots of the angle θ which is determined by formulas (30) as a function of the variable η within the near-wall region. At Re = 57,000, the maximum value of the angle θ, which is approximately equal to 41°, virtually coincides with the observed value of the angle of slope of Λ-vortices (~45°) [5, 6]. At Re = 120,000 and 230,000, the maximum values of the angle θ are nearly half as high. Thus, with increase in the flow velocity the vortex structure of the near-wall region is as if "pressed" to a solid wall; the angle of inclination of vortex filaments to the wall becomes flatter.

The model of near-wall turbulence constructed on the basis of the anisotropy of a turbulent flow is quite satisfactorily confirmed by experimental results.

NOTATION

B, integration constant determined by formula (33); C, integration constant in formulas (13) and (31); e_{ij}, tensor of deformation rates; f_i, density of the external bulk force; F and F_0, free energy of the mass unit of the anisotropic and isotropic fluid, respectively; g_i and G_i, density of the internal and external generalized forces, respectively;

h, half-distance between parallel planes; I, inertia coefficient related to the motion of the landmark vector; k_{11}, k_{22}, k_{33}, and k_{24}, determining constants of the model; N_i, vector determined by formula (9); n_i and $\dot{n}_i$, $\ddot{n}_i$, landmark vector and its time derivatives; p, pressure; p_{ij}, total stresses; $\mathrm{Re} = wh/\nu$, Reynolds number; t_{ij}, turbulent stresses in Sec. 2; u, longitudinal local velocity in formula (13) and Sec. 2; u_i, local velocity of the fluid; x_i, Cartesian coordinates; x, y, Cartesian coordinates in Sec. 2; w, mean velocity of the flow; $w_* = (\tau_\mathrm{w}/\rho)^{1/2}$, dynamic velocity; α_i, vector function entering into Eq. (6); β_{ij}, generalized stresses; γ, function entering into Eq. (8); δ, vortex-layer thickness; δ_{ij}, Kronecker symbol; η, dimensionless distance from a point in the flow to the wall; θ, angle of slope of the landmark vector to the x_1 axis in Sec. 2; κ, von Kármán constant; λ_1, λ_2, μ_1, ..., μ_6, determining constants of the model; ν, kinematic viscosity; ρ, density; σ_{ij}, stresses due to the presence of the structure in the medium; τ_{ij}, viscous stresses; τ_w, modulus of tangential stress on the wall; ω_{ij}, tensor of rotational velocities. Subscripts: i, j, α, and β, natural numbers 1, 2, 3; w, wall.

REFERENCES

1. G. Conte-Bellot, *Ecoulement Turbulent entre Deux Parois Paralleles* [Russian translation], Moscow (1968).
2. V. N. Nikolaevskii, *Prikl. Mat. Mekh.*, **34**, Issue 3, 514–525 (1970).
3. V. N. Nikolaevskii, in: *Vortices and Waves* [in Russian], Moscow (1984), pp. 266–335.
4. B. J. Cantwell, in: *Vortices and Waves* [in Russian], Moscow (1984), pp. 9–79.
5. M. R. Head and P. Bandyopadhaya, *J. Fluid Mech.*, **107**, 297–337 (1981).
6. A. E. Perry and M. S. Chong, *J. Fluid Mech.*, **119**, 173–217 (1982).
7. P. Moin and J. Kim, *J. Fluid Mech.*, **155**, 441–464 (1985).
8. A. E. Perry, S. Henbest, and M. S. Chong, *J. Fluid Mech.*, **165**, 163–199 (1986).
9. Z. Zhang and K. Eisele, *Exp. Fluids*, **24**, 77–82 (1998).
10. N. M. Dmitriev and M. V. Lur'e, *Dokl. Akad. Nauk SSSR*, **225**, No. 4, 775–777 (1975).
11. V. A. Babkin, *Prikl. Mat. Mekh.*, **49**, Issue 3, 401–405 (1985).
12. J. S. Marshall and P. M. Naghdi, *Phil. Trans. Roy. Soc. London*, **A327**, 415–448 (1989).
13. J. S. Marshall and P. M. Naghdi, *Phil. Trans. Roy. Soc. London*, **A327**, 449–475 (1989).
14. J. L. Ericksen, *Trans. Soc. Rheol.*, **5**, No. 1, 23–34 (1961).
15. F. M. Leslie, *Arch. Ration. Mech. Analysis*, **28**, No. 4, 265–283 (1968).
16. E. L. Aéro and A. N. Bulygin, in: *Advances in Science and Technology*, Vol. 7, *Hydromechanics* [in Russian], Moscow (1973), p. 106–213.
17. S. Chandrasekhar, *Liquid Crystals* [Russian translation], Moscow (1980).
18. J. O. Hinze, *Turbulence* [Russian translation], Moscow (1963).